Arraying Nonmagnetic Colloids by Magnetic Nanoparticle Assemblers

Benjamin B. Yellen[1], Randall M. Erb[1], Derek S. Halverson[2], Ondrej Hovorka[2], and Gary Friedman[2]

[1]Department of Mechanical Engineering and Materials Science, Duke University, Durham, NC 27708-0300 USA
[2]Department of Electrical and Computer Engineering, Drexel University, Philadelphia, PA 19104 USA

We review our recent work on the manipulation and assembly of nonmagnetic colloidal materials above magnetically programmable surface templates. The nonmagnetic materials are manipulated by a fluid dispersion of magnetic nanoparticles, known as ferrofluid. Particle motion is guided by a program of magnetic information stored in a substrate in the form of a lithographically patterned template of micromagnets. We show how dynamic control over the motion of nonmagnetic particles can be accomplished by applying rotating external magnetic field. This unexpectedly large degree of control over particle motion can be used to manipulate large ensembles of particles in parallel, potentially with local control over particle trajectory.

***Index Terms*—Assembly, colloid, inverse ferrofluid, patterned magnets.**

I. Introduction

OPTICAL fields [1]–[2] and electrical fields [3]–[4] are widely employed to manipulate colloidal materials, including particles and cells. Magnetic manipulation, on the other hand, is often dismissed because it was thought to require the chemical attachment of magnetic labels to the nonmagnetic materials of interest. We recently demonstrated magnetic manipulation without labeling, by immersing unmodified nonmagnetic materials inside ferrofluid (e.g., a concentrated fluid of magnetic nanoparticles) [5]; the intent being to perform "negative magnetophoresis," which is the manipulation of nonmagnetic particles inside magnetized fluids. Local control over particle trajectories was achieved by defining magnetization patterns in the substrate, serving as a template for generating spatially programmable magnetic field gradients. Meanwhile, global synchronization of particle motion was accomplished by biasing the entire system with spatially uniform pulsating or rotating magnetic field.

In comparison with competing strategies based on optical and electrical fields, magnetic fields offer several inherent advantages making it ideal for colloidal manipulation. For one, the ability to permanently store magnetic information makes ferromagnetic materials an optimal medium for programming highly dense assembly instructions over large areas of the substrate. In contrast, storing programmable electrical field patterns in a substrate is more cumbersome, because it requires sacrificing portions of the substrate for complex wiring patterns and logic for addressing individual electrodes. Optical trapping is also challenging in that it requires patterns of light, produced by arrays of lasers, to generate reconfigurable holographic patterns. Another advantage to magnetic manipulation is that it avoids several undesirable side effects associated with optical or electrical field-based manipulation techniques, which are of particular concern for biological materials and living cells. Optical fields can cause significant heating, and intense electric fields can interfere with various biochemical and biological processes. While the presence of magnetic nanoparticles may also interfere with some biological processes, these side effects are not electromagnetic in origin and can potentially be surmounted by advances in magnetic nanoparticle preparation and surface modification techniques.

In this work, magnetization patterns consisting of discrete Cobalt micromagnets patterned on a substrate are used to control the assembly and transport of nonmagnetic particles ranging in size from <100 nm to several micrometers. Due to the low coercivity of evaporated Cobalt, these micromagnets can be easily remagnetized by application of relatively weak magnetic fields above 60 Oe, thereby serving as a convenient reprogrammable (i.e., remagnetizable) template for flexible manipulation of colloidal particles. Magnetic assembly instructions are transmitted to the nonmagnetic particles through a fluid dispersion of magnetic nanoparticles, known as ferrofluid. These suspensions of large (larger than 50 nm) nonmagnetic particles mixed with smaller (usually below 15 nm) magnetic nanoparticles are known in the literature as "inverse ferrofluids." It should be stressed that in this work, we only present results in which all of the micromagnets have the same magnetization direction at a given time, although the possibility of programming individual micromagnets independently from each other does exist and can be accomplished by optically addressable thermomagnetic recording technology [6].

The rest of the paper will be organized as follows. First, we will briefly discuss the basic principles guiding the assembly and dynamic manipulation of nonmagnetic materials inside magnetic fluids. Next, we will show experimental results from the large scale assembly of nonmagnetic beads onto micromagnet arrays. The ability to program fine-scale robotic operations on nonmagnetic beads will be demonstrated. Thereafter, we will demonstrate the possibility of manipulating ensembles of submicron sized beads using submicron sized magnets. Potential applications of these techniques and major open questions will be noted in the conclusion section.

Digital Object Identifier 10.1109/TMAG.2006.879623

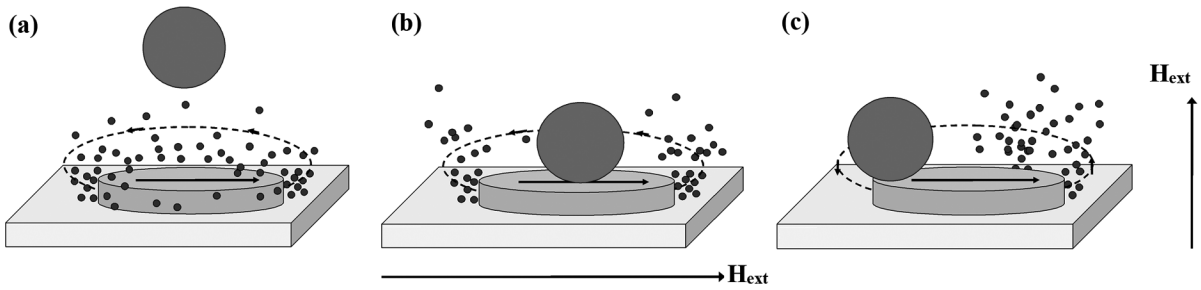

Fig. 1. Schematic illustration of nonmagnetic bead (sphere) immersed in ferrofluid (dots) assembling on top of Cobalt micromagnet (grey disc with arrow denoting trap's magnetization). In (a) no external field is applied, hence, the ferrofluid accumulates near the micro-magnet, whereas the bead is forced vertically away from the micromagnet toward the region of lower magnetic field. In (b) external magnetic field is applied parallel to the micromagnet's magnetization, causing the ferrofluid to accumulate around the edges of the micromagnet where the external field adds to the micromagnet's field (denoted by dotted line with arrow), meanwhile the nonmagnetic particle is pulled directly on top of the micromagnet where the external field subtracts from the micromagnet's field. In (c) external field is applied in the vertical direction, while the micromagnet maintains planar magnetization. This orientation causes the nonmagnetic bead to move to the left edge of the micromagnet, where the external field subtracts from the micromagnet's field, while the magnetic nanoparticles are pulled toward the right edge where the external field and micromagnet's field are additive.

II. Physics of Bead Manipulation

In the linear magnetization regime applicable in this work, the magnetic force $\vec{F}$ on a small colloidal particle depends on the particle volume V, the strength of the field gradient $\nabla\vec{H}$, the permeability of the fluid μ_f, and the screening of the fluid, which is accounted for as the difference in particle magnetization $\vec{M}_p$ with respect to the magnetization of the surrounding fluid $\vec{M}_f$, as given by [7]–[8]

$$\vec{F} = \mu_f V((\vec{M}_p - \vec{M}_f)\cdot\nabla)\vec{H}. \tag{1}$$

In this work, the intent is to apply force to nonmagnetic beads ($\vec{M}_p = 0$), which are suspended inside a strongly magnetized fluid ($\vec{\boldsymbol{M}}_f \neq 0$). To transmit magnetic force, we use a suspension of magnetic nanoparticles (i.e., ferrofluid) as the carrier fluid. Due to the small size of the magnetic nanoparticles and their substantial random motion, the fluid can be described by a continuum model, and the average fluid magnetization represented as the product of the nanoparticle magnetization $\vec{\boldsymbol{M}}_{\rm np}$ and the volume fraction of nanoparticle material inside the fluid C. When interactions between nanoparticles can be neglected, the volume magnetization of the nanoparticle is assumed to be linearly proportional to the external magnetic field as given by [9]

$$\vec{\boldsymbol{M}}_f = \langle\vec{\boldsymbol{M}}\rangle = \vec{\boldsymbol{M}}_{\rm np}C = \chi\boldsymbol{C}\vec{\boldsymbol{H}}, \qquad \chi = \frac{\mu_0 V M_s^2}{3k_B T} \tag{2}$$

where χ is the initial magnetic susceptibility of the nanoparticle, M_s is its saturation magnetization of the nanoparticles, k_B is Boltzmann's constant, and T is the absolute temperature in Kelvin.

Equation (1) demonstrates that nonmagnetic particles placed into a paramagnetic fluid behave effectively as diamagnetic particles placed in a nonmagnetic fluid. For this reason, the nonmagnetic particles ($\vec{M}_p = 0$) are attracted to the regions of magnetic field minima. These regions of magnetic field minima act like traps for the nonmagnetic particles. The position of these traps is jointly determined by the pattern of magnetization on the substrate and by the external magnetic field. In the case when no external field is applied (e.g., the magnetic field is produced solely by an array of micromagnets patterned on a substrate), the magnetic field minima regions are located far from the magnetic pattern, and the nonmagnetic beads are forced to levitate well above the substrate, as shown in Fig. 1(a). However, when external field is applied to the system, the pattern of traps (regions of magnetic field minima) are shifted toward the substrate, specifically to the positions where the micromagnet's field subtracts from the external magnetic field, as shown in Fig. 1(b) and (c). Using this phenomenon, colloidal particles and molecules have been concentrated on the surface and then redispersed by turning the external magnetic field ON and OFF [5]. In addition, we have shown that by reorienting the external field relative to the micromagnet's magnetization, the pattern of traps can be shifted to different positions. By continuously shifting the traps in an externally rotating field, nonmagnetic particles have been transported linearly across the surface from one micromagnet to the next [5], or shuttled back and forth on the same micromagnet.

The intrinsic advantage to using magnetic fields, over optical or electrical fields for colloidal manipulation, is that magnetic fields can store a higher spatial energy density than is achievable by electric fields, which are limited by dielectric breakdown and induced fluid movement. Consider that the ratio of energy density between applied magnetic and electric fields which is: $\mu\boldsymbol{H}^2/\varepsilon\boldsymbol{E}^2 = c^2\boldsymbol{B}^2/\boldsymbol{E}^2$. Assuming that magnetic flux density of 1 T can be generated (this is achievable with permanent magnets), the electric field intensity needed to obtain an equivalent energy density is approximately 10^7–10^8 V/m, for typical values of fluid dielectric permittivity. This represents an extremely strong electric field, which causes substantial heating and flows in aqueous solutions, and can lead to dielectric breakdown in many materials [10]. For this reason, the electric fields used in dielectrophoresis are much smaller, typically below 10^6 V/m, and the resulting electric forces are at least an order of magnitude weaker than similar forces obtained in magnetic manipulation. Since magnetism enables the manipulation of substantially smaller particles than is possible by electrical or optical fields, the previous calculation motivates the preference for magnetic forces in arranging micro and nanoparticles onto surfaces.

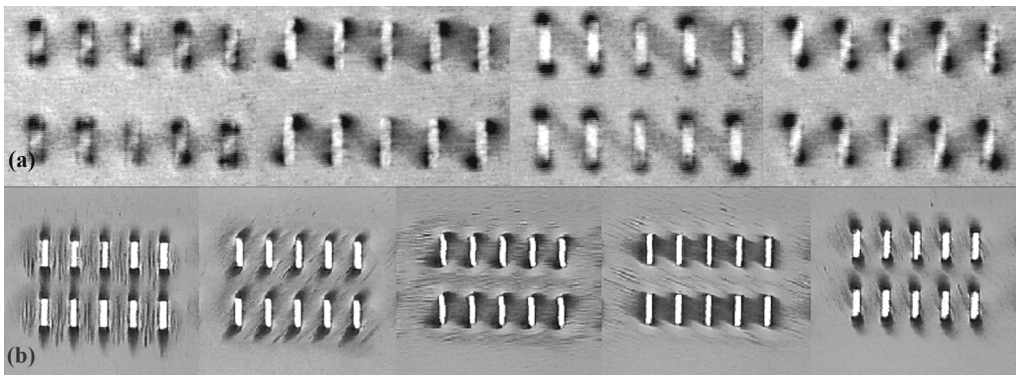

Fig. 2. Sequence of images taken over 0.5 s demonstrates the ability to shift ferrofluid aggregates around the magnetic traps with in-plane rotating magnetic field. The micromagnets have dimensions of 4×20 μm and they are spaced 20 μm apart. Image (a) shows the weak field mode, in which magnetic field of <50 G is rotating in the plane, causing the ferrofluid aggregates to circulate around each of the micromagnet's poles. These photographs are evidence that the micromagnets retain fixed magnetization throughout the course of the experiment. Image (b) shows the ferrofluid aggregation in the strong field mode where magnetic field of >100 G is rotating in the plane, causing the ferrofluid to circulate around the trap circumference; which is evidence that the micromagnets' magnetizations are rotating with the applied field.

III. Materials and Methods

Experimental work employed thin Cobalt film (ranging from 50–100 nm thick) patterned on Silicon or glass wafers into different shapes and geometrical arrangements. The film was produced by conventional metal evaporation and lift-off techniques described elsewhere [11]. The saturation magnetization of the patterned micromagnets was measured to be roughly 1 T, in accordance with previously reported properties of patterned 50-nm thick Cobalt film [12]. The planar dimensions of the micromagnets ranged from 200 nm to 1 mm. Due to the extreme diversity in the size and shape of the micromagnets used in experiments, we will indicate in the results section the type of magnetic pattern used for each particular experiment. Magnetic nanoparticles of roughly 100 Å diameter were purchased from Ferrotec in aqueous-based solution (i.e., ferrofluid) with particle content occupying 1.1% volume fraction of the fluid. The ferrofluid had initial magnetic susceptibility of 0.24, and viscosity of 5 cP. Monodisperse nonmagnetic colloidal particles ranging from 100 nm to 5 μm were purchased from Duke Scientific as an aqueous suspension with particle content occupying 1% volume fraction of the fluid. The nonmagnetic beads contained a fluorescent dye so that their movements could be tracked by fluorescent microscopy. The commercially obtained nonmagnetic beads were coated with steric and charged groups which improved the colloidal stability, however, some aggregation of the particles inside the ferrofluid was observed. A drop of the ferrofluid/particle mixture was placed directly on the wafer, and the fluorescent particles were moved about the surface by externally pulsating or rotating magnetic field.

Oscillating or rotating magnetic field was produced using three orthogonal sets of solenoid coils with iron cores arranged with respect to the wafer. The arrangement of coils was designed to ensure control over the magnetic field in three orthogonal directions (i.e., the x, y, and z directions). Reasonably uniform magnetic fields could be applied in the range of 0–200 G in any direction with this setup. Each set of coils was connected to an independent channel, and their waveforms were programmed in DASYLAB 7.0 software to produce controlled magnetic field rotation in the range of 0 to 40 Hz. The magnetic field was measured with a hand-held Hall probe (Lakeshore Cyrotronics).

In order to best observe the bead assembly process, we observed bead motion with a Leica DM LFS microscope adjusted for optimal contrast. A thin fluid film was created by sandwiching a drop of ferrofluid between a glass slide and the magnetized substrate. The typical thickness of the fluid film was measured to be 5–10-μm, however, in some cases, a spacer layer consisting of 5-μm thick posts or walls, fabricated in SU-8 2005 photoresist, was overlaid on top of the micromagnet array in order to increase the thickness of the fluid film.

IV. Results

A. Ferrofluid Movement Above Micromagnets

We initially studied the motion of magnetic nanoparticles in the absence of the nonmagnetic beads. When the external field changes slowly (e.g., below 10 Hz), local aggregates of magnetic nanoparticles moved about the substrate, following synchronously with the traveling regions of magnetic field maxima. Depending on the coercivity of the micromagnets, two modes of ferrofluid motion were observed. In one mode, when the external field was sufficiently weak, the micromagnets retained fixed magnetization, which resulted in ferrofluid aggregates rotating around the fixed poles of the micromagnets. In this case, the ferrofluid aggregates sweep over the top of the micromagnet during each field rotation as shown in Fig. 2(a). This mode was only observed in rotating magnetic field weaker than 50 G, since the coercivity of the micromagnets was measured to be around 60 G. In the second mode, the external field was sufficiently strong to cause rotation of the micromagnet's magnetization, and this resulted in the ferrofluid aggregates moving around the circumference of the micromagnets, as shown in Fig. 2(b).

B. Bead Assembly in Strong Field Mode

When studying the motion of nonmagnetic beads, we found that the strong field mode is better suited for the assembly of these beads, since the traps (regions of field minima) are always located in the middle of the micromagnets. However, we have

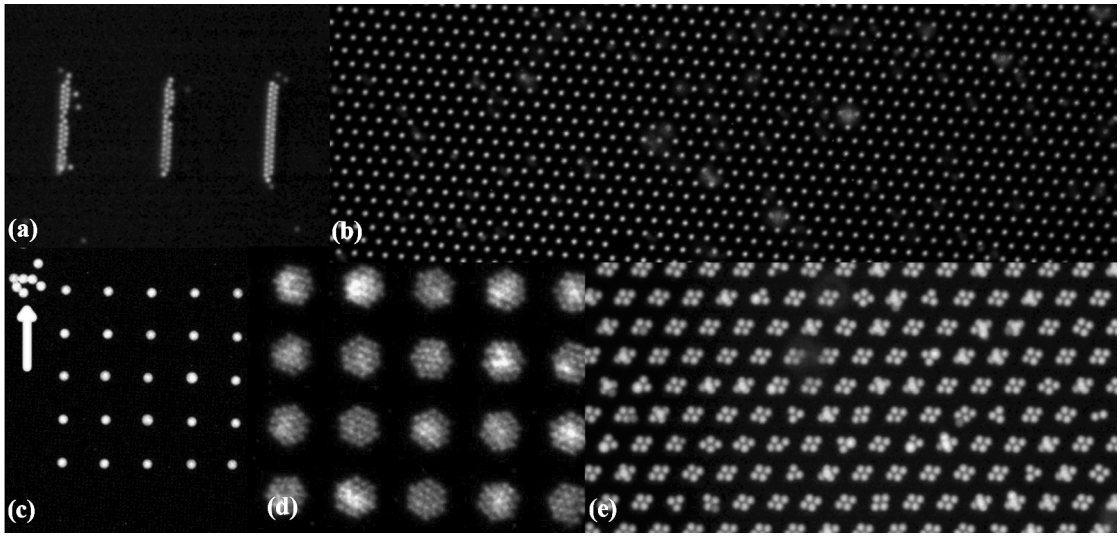

Fig. 3. Patterns shown in (a)-(e) consist of micron-sized Cobalt micromagnets capturing nonmagnetic beads. In (a), the structures consist of 4×20 μm rectangular magnets spaced 20 μm apart, and they are used to capture 1 μm nonmagnetic beads. In (b)-(e) the structures consist of 5 μm circular magnets. The circular magnets are arranged in either triangular lattices in (b) and (e) with periodicity of 8 μm, or in rectangular lattices in (c)-(d) with periodicity of either 30 μm in (c) or 8 μm in (d). The number of beads which can stably fit on each micromagnet depends on the relative size of the bead with respect to the trap. For example, when the beads are 3 μm as shown in (b) or 5 μm as shown in (c), each trap can capture only one bead apiece, whereas if the beads are 1 μm as shown in (d) or 2 μm as shown in (e), several beads can stably fit on each micromagnet. In (c) an arrow is provided to indicate some contamination that was produced by magnetic alignment marks in the upper-left-hand corner. Images (d) and (e) were taken after the fluid had dried, whereas images (a)-(c) were taken while still immersed in the fluid.

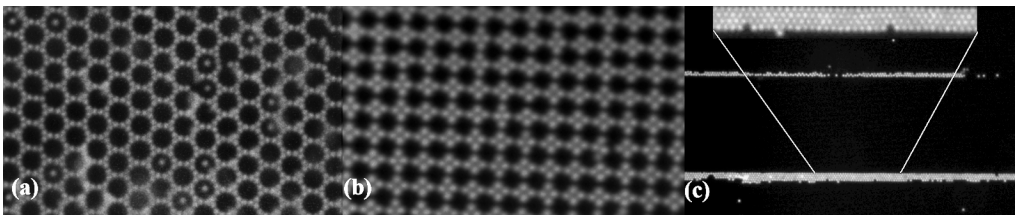

Fig. 4. Patterns shown in (a) and (b) were produced in uniform Cobalt film patterned with an array of 5-μm holes. The distance between the center of the holes was 8 μm, which are arranged in either (a) triangular or (b) rectangular arrays. The pattern in (c) consists of a uniform Cobalt film patterned with an array of lines 100 μm wide. The beads assembling on each of these patterns have (a) 2, (b) 3, and (c) 1 μm diameters. Images (c) were taken while inside the fluid, whereas images (a) and (b) were taken after the fluid had dried.

found that the weak field mode is more conducive to programming fine motion of nonmagnetic beads on the surface, as will be demonstrated in later sections. Initial experiments have demonstrated that large arrays of micron-sized beads can be assembled into the micromagnets inside a weakly concentrated solution of magnetic nanoparticles (less than 1% by volume). Even in static magnetic field, a high degree of control over bead assembly can be achieved; however, bead aggregation was a major problem due to the lack of relative motion. When pulsating or rotating field was applied, the movement of the magnetic nanoparticles did not permit more than one bead to assemble in any one trap and created steady-state particle patterns as shown in Figs. 3 and 4. Strong in-plane rotating magnetic field was used to rotate the micromagnet's magnetization and promote the formation of a stable energy minimum for each particle, located directly on top of the micromagnet as shown in Fig. 1(b) (e.g., where the micromagnet's field subtracted from the external field). This configuration led to reliable packing of nonmagnetic beads only in the middle of the micromagnets, whereas beads approaching other areas of the surface were swept away by the relative fluid motion caused by the circulation of magnetic nanoparticles around the micromagnets.

A combination of related phenomena is probably responsible for disrupting the formation of a secondary layer of beads in this experimental configuration. When external field is applied parallel to the substrate, the beads are repelled from each other magnetically and are unlikely to chain up along the direction normal to the substrate, thereby preventing beads from piling directly on top of one another. On the other hand, the beads that were not directly on top of the micromagnets were swept away by the circulation of ferrofluid around the micromagnets, thereby preventing beads from chaining up parallel to the substrate. The richness of attractive and repulsive interactions nearby the substrate allows for a variety of colloidal patterns (both close packed and separated) to be produced with very few defects. This technique also provides significant flexibility compared to other self-assembly methodologies based on particle sedimentation [13], electrostatic trapping [14], or morphological templating [15].

Fig. 3 shows the assembly of beads on micron-sized micromagnets patterned on a silicon substrate. Fig. 4 shows the assembly of beads on the inverse pattern, consisting of a continuous Cobalt film containing an array of holes of different shapes and sizes. In this arrangement, the beads are still attracted on top

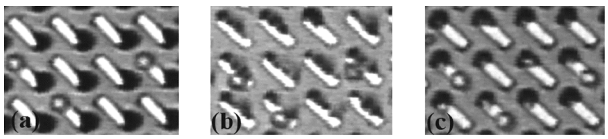

Fig. 5. Micromagnets were initially magnetized along their long axis. In plane weak rotating magnetic field (50 G, 1 Hz) is combined with a dc vertically directed bias field of 100 G, causing the nonmagnetic to assemble on the upper-left-hand corner of the rectangular micromagnets, as shown in (a). When the dc bias field is switched to -100 G, the beads were transferred to the lower-left-hand corner of the micromagnets, as shown in (c).

of the magnetic film; however, this trap pattern promoted the assembly of features which resemble honeycomb structures.

C. Programmable Assembly

In the weak field mode, controlled arrangement of beads on the micromagnets was rarely observed when purely in-plane rotating magnetic field was applied to the substrate. However, the weak field mode is conducive to performing fine robotic operations on particles, by employing the information stored in the magnetization pattern. For example, when a static magnetic field is applied in the vertical direction, the ferrofluid accumulates preferentially nearby one of the micromagnet's poles, and avoid the other pole as illustrated schematically in Fig. 1(c), [16]. The nonmagnetic beads are attracted to a stable region of magnetic field minima located at the pole opposite of the ferrofluid aggregates. It was observed that a combination of a rotating in-plane magnetic field and static vertical field provided the best control over the assembly of nonmagnetic beads in this case. The beads can be transferred from one side of the micromagnet to the other by simply reversing the static vertical magnetic field, as shown in Fig. 5.

D. Nanoscale Assembly

Magnetic nanoparticle assembly experiments were also performed with magnets and beads with submicron dimensions [17]. Submicrometer features were first defined in PMMA photoresist, followed by evaporation of 50-nm thick Cobalt film. The resulting Cobalt magnets had dimensions ranging from 200 to 1000 nm. Nonmagnetic beads with diameters ranging from 100 to 300 nm were manipulated by the various Cobalt magnet patterns inside 1% concentrated ferrofluid solution and using external fields of $<$500 G in magnitude. At this size scale, bead capture is still possible; however, Brownian motion has a stronger influence over bead motion. One exemplary image of nano-bead manipulation is provided in Fig. 6.

The probability for capturing a nano-bead from suspension can be estimated by comparing the magnetic potential energy of a nano-bead held in a trap with thermal fluctuation energy, k_BT. A rough estimate of the magnetic energy is obtained by integrating the force equation in (1), leading to the following expression for the energy of nonmagnetic bead placed inside a homogeneous magnetic fluid of permeability, μ_f:

$$U_{\mathrm{mag}} = \frac{3}{2}\mu_f V_p \left(\frac{\mu_0 - \mu_f}{\mu_0 + 2\mu_f}\right)\left(H_{\mathrm{ext}}^2 - (H_{\mathrm{ext}} + H_{\mathrm{trap}})^2\right). \tag{3}$$

Equation (3) indicates that an upper limit of the potential energy depth of the trap is obtained when the field of the micro-

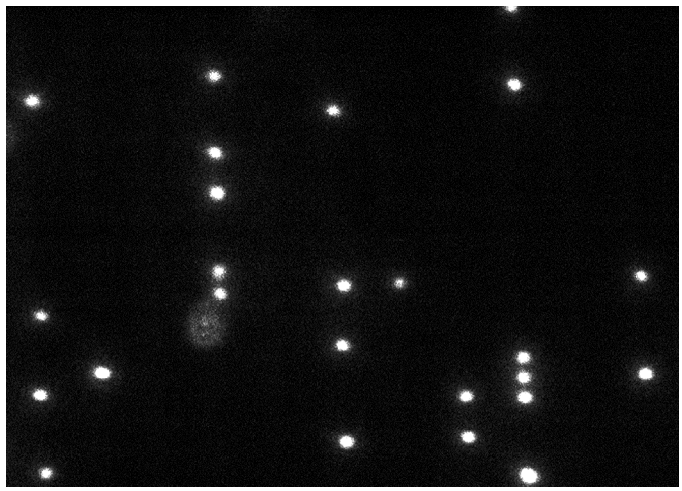

Fig. 6. This fluorescent micrograph shows the assembly of 300-nm beads on an array of 340 $\times$ 1000 nm Cobalt micromagnets spaced in a rectangular array. Uniform 400-G magnetic field was applied to the traps to encourage the assembly of nonmagnetic nano-beads.

magnet cancels the external field at the trap's location. This upper limit is proportional to the square of the external field. Assuming the ferrofluid permeability is $\mu_f \approx 1.5\mu_0$, which is a reasonable estimation based on data taken from commercial vendors of typical aqueous ferrofluid (Ferrotec, Nashua, NH), (3) leads to an upper bound of the potential energy well of $\sim 2000 k_BT$ for beads of 300 nm diameter, and $\sim 10 k_BT$ for beads of 50 nm diameter when the external field is 500 Oe. Hence, these estimates indicate that beads with a $<$100-nm diameter can also be captured by micromagnets, however, their escape probability is much higher than for beads with a $>$100-nm diameter.

V. Conclusion

The main purpose of this work was to develop methods for magnetically manipulating materials in a programmable fashion without requiring their attachment to magnetic particle carriers, which is the most common magnetic manipulation scheme [18], [19]. A number of potential applications are envisioned for the techniques developed in this work. For example, the ability to bring nonmagnetic components toward a surface by cycling the magnetic field ON and OFF may be used to assist biological sensing applications, such as in bringing target molecules, viruses, or bacteria to sample different sensor regions more quickly than is possible by diffusion alone. The particle assembly techniques may also assist the fabrication of a variety of emerging devices that require the precise arrangement of biological materials [20], colloidal particle arrays for photonic applications [21], or nanotubes and nanowire for future electronic components [22] or display elements [23].

The proposed method may have certain limitations and a number of open questions remain. One important issue not addressed by this work is the method for fixing the materials onto the substrate once they are assembled. Another open question is the ability to remove the ferrofluid after the assembly process and the possible effects of ferrofluid on living systems, such as proteins, cells, and viruses. The compatibility of the

chosen ferrofluid with biological materials was not tested in the reported experiments. As mentioned in the introduction, magnetic recording techniques will be needed for independent control over particle trajectories and assembly patterns with local precision. Conventional recording methodology may require some rethinking for such applications. We hope to address some of the open questions concerning the proposed magnetic manipulation and assembly methods in future work.

ACKNOWLEDGMENT

This work was supported in part by the National Science Foundation NIRT under Award 0304453 and by the Department of Defense Graduate Fellowship, for one of the authors.

REFERENCES

[1] E. R. Dufresne and D. G. Grier, *Rev. Sci. Instr.*, vol. 69, pp. 1974–1977, 1998.
[2] J. E. Curtis, B. A. Koss, and D. G. Grier, *Opt. Commun.*, vol. 207, pp. 169–175, 2002.
[3] O. D. Velev, B. G. Prevo, and K. H. Bhatt, *Nature*, vol. 426, pp. 515–516, 2003.
[4] Z. Suo and W. Hong, *Proc. Nat. Acad. Sci.*, vol. 101, pp. 7874–7879, 2004.
[5] B. B. Yellen, O. Hovorka, and G. Friedman, *PNAS*, vol. 102, pp. 8660–8664, 2005.
[6] M. Mansuripur, *The Physical Principles of Magneto-Optical Recording*. Cambridge, U.K.: Cambridge Univ. Press, 1995.
[7] A. T. Skjeltorp, *Phys. Rev. Lett.*, vol. 51, pp. 2306–2309, 1983.
[8] G. Helgesen, P. Pieranski, and A. T. Skjeltorp, *Phys. Rev. A.*, vol. 41, pp. 7271–7280, 1990.
[9] O. Hovorka, B. B. Yellen, N. Dan, and G. Friedman, *J. Appl. Phys*, vol. 97, pp. 10Q306–3, 2005.
[10] A. Ashkin and J. Dziedzic, *Science*, vol. 235, pp. 1517–1520, 1987.
[11] M. Madou, *Fundamentals of Microfabrication*. Boca Raton, FL: CRC, 1997.
[12] G. J. Parker and C. Cerjan, *J. Appl. Phys*, vol. 87, pp. 5514–5516, 2000.
[13] A. van Blaaderen, R. Ruel, and P. Wiltzius, *Nature*, vol. 385, pp. 321–324, 1997.
[14] J. B. Aizenberg, P. V. Braun, and P. Wiltzius, *Phys. Rev. Lett.*, vol. 84, pp. 2997–3000, 2000.
[15] Y. Yin, Y. Lu, B. Gates, and Y. Xia, *J. Amer. Chem. Soc.*, vol. 123, pp. 8718–8729, 2001.
[16] B. B. Yellen, G. Fridman, and G. Friedman, *Nanotechnol.*, vol. 15, pp. S562–565, 2004.
[17] D. S. Halverson, B. B. Yellen, and G. Friedman, *J. Appl. Phys.*, vol. 99, no. 8, p. 08P504, 2006.
[18] M. A. M. Gijs, *Microfluid Nanofluid*, vol. 1, pp. 22–40, 2004.
[19] B. B. Yellen and G. Friedman, *Langmuir*, vol. 20, pp. 2553–2559, 2004.
[20] S. Fodor, R. P. Rava, X. C. Huang, A. C. Pease, C. P. Holmes, and C. L. Adams, *Nature*, vol. 364, pp. 555–557, 1993.
[21] G. A. Ozin and S. M. Yang, *Adv. Func. Mater.*, vol. 11, no. 2, pp. 95–104, 2001.
[22] X. Duan, Y. Huang, Y. Cui, J. Wang, and C. M. Lieber, *Nature*, vol. 409, pp. 66–69, 2001.
[23] H. O. Jacobs, A. R. Tao, A. Schwartz, D. H. Gracias, and G. M. Whitesides, *Science*, vol. 5566, pp. 323–325, 2002.

Manuscript received March 13, 2006 (e-mail: yellen@duke.edu).